# Enantioselective Synthesis of Polysubstituted Spiro-nitroprolinates Mediated by a (R,R)-Me-DuPhos·AgF-Catalyzed 1,3-Dipolar Cycloaddition

Alberto Cayuelas,[†,‡,§] Ricardo Ortiz,[†] Carmen Nájera,[†,‡] José M. Sansano,*[,†,‡,§] Olatz Larrañaga,[‡,‖] Abel de Cózar,[‡,‖,⊥] and Fernando P. Cossío*[,‡,‖]

[†]Departamento de Química Orgánica, Facultad de Ciencias, Universidad de Alicante, 03080 Alicante, Spain
[‡]Centro de Innovación en Química Avanzada (ORFEO−CINQA), Universidad de Alicante, 03080 Alicante, Spain
[§]Instituto de Síntesis Orgánica (ISO), Universidad de Alicante, 03080 Alicante, Spain
[‖]Departamento de Química Orgánica I, Facultad de Química, Universidad del País Vasco, P. K. 1072, E-20018 San Sebastián, Spain
[⊥]IKERBASQUE, Basque Foundation for Science, 48011 Bilbao, Spain

S *Supporting Information*

ABSTRACT: The synthesis of constrained spirocycles is achieved effectively by means of 1,3-dipolar cycloadditions employing α-imino γ-lactones as azomethine ylide precursors and nitroalkenes as dipolarophiles. The complex formed by (R,R)-Me-DuPhos **18** and AgF is the most efficient bifunctional catalyst. Final spiro-nitroprolinates cycloadducts are obtained in good to moderate yields and both high diastereo- and enantioselectivities. Density functional theory (DFT) calculations supported the expected absolute configuration as well as other stereochemical parameters.
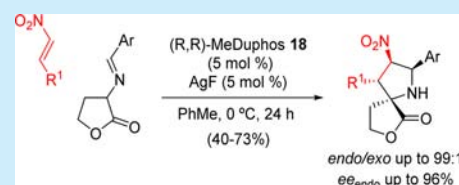
The importance of having a wide number of enantiomerically enriched sterically congested polysubstituted organic compounds is continuously increasing. Many scientific areas need all these functionalized structures for their specialized studies. Along this line, optically active polysubstituted nitroprolinates have emerged since 2005 as promising therapeutic agents.[1] For example, molecules **1** (Figure 1) are important
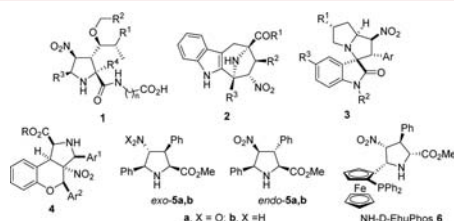

Figure 1. Nitroprolinates with synthetic or biological applications.

inhibitors of $\alpha_4\beta_1$-integrin-mediated hepatic melanoma and in a murine model of colon carcinoma metastasis, as well as exhibits potent antiadhesive properties in several cancer cell lines.[2,3] Bicyclic heterocycles **2**, containing an atropane scaffold, have been found as novel inhibitors of skin cancer.[4] Spirooxindoles **3** increased the mortality of zebrafish embryos[5] while molecules **4** with a benzopyran skeleton were successfully tested as antimycobacterials against the *M. tuberculosis* H37Rv strain.[6] Besides, the most simple 4-nitroprolines *exo*-**5**, and *endo*-**6** have been recently used as chiral organocatalysts in aldol reactions.[7] Michael-type addition of ketones to nitroalkenes was successfully run in the presence of *exo*-**5b** (X = H),[8] obtaining good to

excellent diastereoselectivity and high enantiomeric ratios. A family of enantiopure tetrasubstituted nitroprolinate surrogates have been designed as scaffolds for proteasome inhibitors with high medicinal prospects.[9] In addition, the NH-D-EhuPhos ligand **6** has been efficiently employed in the 1,3-dipolar cycloadditions (1,3-DC)[10] to yield nitroprolines and structurally rigid spirocompounds from chiral γ-lactams.[11,12]

Grigg et al. reported the Ag-promoted racemic and diastereoselective 1,3-DC involving homoserine derived imino esters **7**[13] and nitroalkenes **8** obtaining spirolactones **9** as major products (Scheme 1).[14] The asymmetric approach to this

Scheme 1. Racemic 1,3-DC between Iminolactones 7 and Nitroalkenes 8
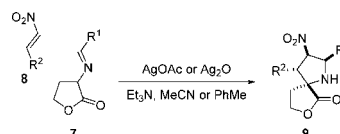
molecules was performed by the employment of organocatalysts. Michael adducts could be isolated in a first step. A second treatment with DBU afforded enantiomerically enriched endo-cycloadducts **9** in good yields.[15] These homoserine-lactone surrogates are a class of signaling molecules involved in the so-called bacterial quorum sensing.[16]

In this work, with the idea of combining structural rigidity and enantiomerically enriched nitroprolinates, we report the direct enantioselective synthesis of these attractive intermediates **9**.[17−19]

For the optimization of the reaction privileged ligands **11−20** were tested in the silver-catalyzed 1,3-DC between imino lactone **7a** and β-nitrostyrene **8a**. Although we used L-homoserine lactone as starting material to prepare dipole precursors **9**, the chiral information contained in these compounds is not relevant (*vide infra*). (*S*)-Segphos **13**, (*S*)-Binap **10**, and its derivatives **11** and **12** afforded very low enantiomeric ratios (although high diastereoselectivity) of the major *endo*-cycloadduct, with *ent*-**9aa** AgTfa (Tfa = trifluoroacetate) and AgF being the most appropriate silver(I) salts (Table 1, entries 1−6). Then, phosphoramidites **14−17** were evaluated next. When the reaction was run in the absence of triethylamine using the (*R*$_a$,*S*,*S*)-**14**·AgF

complex, better results were recorded (Table 1, entries 7 and 8). Other silver salts in combination with phosphoramidite **14**, useful in other 1,3-DC with nitroalkenes,[20] such as AgOTf, AgOBz, AgOAc, and Ag$_2$CO$_3$,[21] were assayed but never improved the results obtained with AgF (Table 1, entries 9−15). Phosphoramidites **15−17** gave poor enantioselectivities (Table 1, entries 13−15). However, the (*R*,*R*)-Me-DuPhos **18**·AgF complex furnished *endo*-**9aa** in 99:1 dr and 86:14 er. Chiral ferrocenyl ligands **19** and **20** did not give better results (Table 1, entries 16−18). The effect of the temperature was considered, and the enantiomeric ratio could be increased up to 90:10 when the reaction was performed at 0 °C rather than when the reaction was carried out at −20 °C (Table 1, entries 19 and 20). The high *endo:exo* ratio achieved in entry 16 of Table 1 (99:1) versus the 3:1 reported in the literature for the racemic mixture is remarkable.[14]
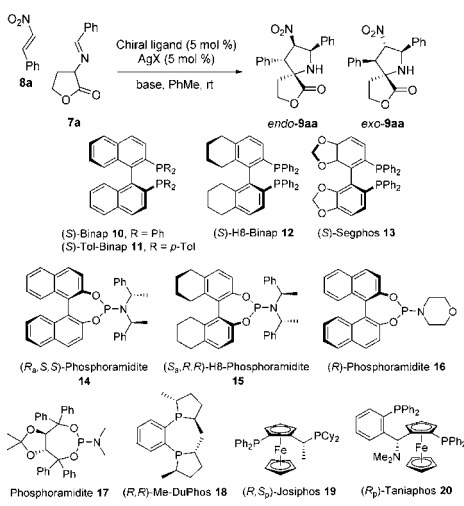
The possible structure of the catalyst involved in the process was studied. For a 1:1 mixture of (*R*,*R*)-Me-DuPhos **18** and AgF, a ^{31}P NMR experiment (in deuterated chloroform) revealed two doublets at 22.66 ppm (J_{Ag109} = 256 Hz and J_{Ag107} = 222 Hz) and ESI-MS afforded an M$^+$ = 719 corresponding to the (**18**)$_2$·Ag cluster. Analogous ^{31}P NMR and ESI-MS spectra were recorded when a 2:1 mixture of (*R*,*R*)-Me-DuPhos **18** and AgF was prepared. Another ^{31}P NMR experiment was performed by addition of **7a** to the preformed 1:1 complex (*R*,*R*)-Me-DuPhos **18**:AgF, but no signals were detected. At this point, we performed the reaction using the Table 1 entry 16 conditions with the (**18**)$_2$· AgF complex generated *in situ*. The reaction was very slow, and almost racemic *endo*-**9aa** was obtained with less than 5% conversion after 1 d.

The scope of the reaction was next investigated. (*R*,*R*)-Me-DuPhos **18** and AgF[22] were mixed and stirred for 30 min, and the imino ester **7** was added at 0 °C followed by the nitroalkene **8**. Unsubstituted and 2-, 3-, or 4-substituted aryl groups of the nitrostyrene molecule afforded in relatively good yields (45−54%) **9ac−ae** cycloadducts with high diastereoselectivity and moderate to high enantiomeric ratios (Table 2, entries 1−4). 2-Furyl derivative **8e** and alkyl substituted nitroalkenes **8f−g** afforded higher er and good chemical yields with modest diastereoselectivity (Table 2, entries 5−7). In these examples run with alkylated nitroolefins, the diastereoselectivity was higher than the 1:1 obtained in the literature.[14] A modification of the aryl group of imino lactone **7** gave, in general, similar chemical yields, and higher diastereo- and enantiomeric ratios of products **9** (Table 2, entries 8−15). 2-Methylphenyl surrogate **7b** was also an appropriate precursor giving **9ba** as only one diastereoisomer although with a low enantiomeric ratio (80:20, Table 2, entry 8).

Theoretical calculations within the density functional theory (DFT) framework[23] were carried out in order to further assess the origins of the observed enantio- and diastereoselectivity in the 1,3-DC of **7a** and nitroalkene **8** catalyzed by (*R*,*R*)-MeDuPhos **18**· AgF. This latter computational method has been demonstrated to be a useful tool for the analysis of the stereochemical outcome observed in 1,3-DC, especially in reactions catalyzed by chiral silver(I) complexes.[19b,22b,24] Moreover, we demonstrated in previous works that the enantioselectivity stems from the coordination pattern in the azomethine ylide and the effective blockage of one of the prochiral faces by the chiral ligand in the initial reactive complex.[25]

Our calculations on the initial N-metalated **INT1** reactive complex show that the silver(I) atom presents a tetrahedral environment where the coordination sphere is saturated by the carbonylic oxygen atom, the nitrogen atom of the azomethine ylide, and the two phosphorus atoms of the ligand **18** (see
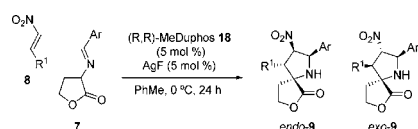
Table 1. Optimization of Reaction Conditions of 1,3-DC of 7a and 8a

entry	ligand	AgX	base	conv (%)^a	endo:exo^a	er^{b,c}
1	(*S*)-**10**	AgTfa	TEA	>98	93:7	45:55
2	(*S*)-**10**	AgF	TEA	>98	89:11	45:55
3	(*S*)-**10**	AgTfa^c	TEA	>98	93:7	36:64
4	(*S*)-**11**	AgF	TEA	>98	96:4	50:50
5	(*S*)-**12**	AgF	TEA	>98	98:2	31:69
6	(*S*)-**13**	AgF	TEA	>98	98:2	20:80
7	(*R*$_a$,*S*,*S*)-**14**	AgF	TEA	>98	88:12	73:27
8	(*R*$_a$,*S*,*S*)-**14**	AgF	−	>98	90:10	78:22
9	(*R*$_a$,*S*,*S*)-**14**	AgOTf	−	>95	84:16	66:34
10	(*R*$_a$,*S*,*S*)-**14**	AgOBz	−	>98	91:9	65:35
11	(*R*$_a$,*S*,*S*)-**14**	AgOAc	−	>98	86:14	66:34
12	(*R*$_a$,*S*,*S*)-**14**	Ag$_2$CO$_3$	−	>98	92:8	70:30
13	(*S*$_a$,*R*,*R*)-**15**	AgF	−	>98	76:24	36:64
14	(*R*)-**16**	AgF	−	>98	99:1	70:30
15	**17**	AgF	−	>95	92:8	37:63
16	(*R*,*R*)-**18**	AgF	−	>95	99:1	86:14
17	**19**	AgF	−	>95	79:21	66:34
18	**20**	AgF	−	>20	−	−
19	(*R*,*R*)-**18**	AgF^d	−	>95	99:1	90:10
20	(*R*,*R*)-**18**	AgF^e	−	>90	99:1	88:12

^{a}Determined by ^{1}H NMR of the crude reaction mixture. ^{b}Determined by HPLC using chiral coated columns, *endo*-**9aa**:*ent*-**9aa** er. ^{c}Reaction performed at −50 °C during 50 h. ^{d}Reaction performed at 0 °C during 50 h. ^{e}Reaction performed at −20 °C.

**Table 2. Scope of the Enantioselective 1,3-DC of 7 and Nitroalkenes 8**

entry	7, Ar	8, R^1	9	yield (%)^a	endo:exo^b	er^{c,d}
1	7a, Ph	8a, Ph	9aa	65	99:1	90:10
2	7a, Ph	8b, 4-FC$_6$H$_4$	9ab	45	99:1	80:20
3	7a, Ph	8c, 2-BrC$_6$H$_4$	9ac	50	95:5	75:25
4	7a, Ph	8d, 3-BrC$_6$H$_4$	9ad	54	95:5	95:5
5	7a, Ph	8e, 2-Furyl	9ae	71	99:1	92:8
6	7a, Ph	8f, Cy	9af	65	78:22	96:4
7	7a, Ph	8g, Bu^i	9ag	68	74:26	93:7
8	7b, 2-MeC$_6$H$_4$	8a, Ph	9ba	50	95:5	75:25
9	7c, 3-MeC$_6$H$_4$	8a, Ph	9ca	73	95:5	93:7
10	7d, 4-MeC$_6$H$_4$	8a, Ph	9da	51	99:1	93:7
11	7e, 4-MeOC$_6$H$_4$	8a, Ph	9ea	52	97:3	94:6
12	7f, 4-BrC$_6$H$_4$	8a, Ph	9fa	40	99:1	98:2
13	7g, 2-Naphthyl	8a, Ph	9ga	45	99:1	93:7
14	7h, 2-Furyl	8a, Ph	9ha	51	99:1	80:20

^{a}Isolated yield after purification (flash silica gel). ^{b}Determined by ^{1}H NMR of the crude reaction mixture. ^{c}Determined by HPLC using chiral coated columns. ^{d}Values for compounds endo-9.

Supporting Information). This coordination pattern implies an effective blockage of the (1Si,3Re) prochiral face, thus prompting the preferential formation of cycloadducts endo-9 and exo-9 over its enantiomeric counterparts ent-endo-9 and ent-exo-9. At this stage the chiral information contained in the α-amino-γ-butyrolactone moiety is destroyed because of the formation of the azomethine ylide. Therefore, any source of chiral information relies on the chiral ligand (Figure 3).

Exploration of the Gibbs free energy surface shows that these 1,3-DC are not concerted but stepwise.[26] The first step consists of a Michael-type nucleophilic attack on the α,β-unsaturated nitro derivative to yield an intermediate INT2 that leads to formation of the corresponding cycloadduct by an intramolecular Mannich-like ring closure step. The main geometric features and relative energies of the stationary points corresponding to the first step of the 1,3-DC between 7a and nitroalkene 8a catalyzed by (R,R)-MeDuPhos 18·Ag are gathered in Figure 2.

Our results showed that TS1 and TS2, associated with the formation of cycloadduct endo-9 and its enantiomer ent-endo-9, are less energetic than TS3 and TS4 (associated with formation of exo-9 and ent-exo-9) due to a favorable Coulombic interaction between the nitro moiety of 8 and the silver atom in the former. This favorable interaction, associated with an endo approach, results in a theoretical diastereomeric endo-9:exo-9 ratio of 99:1, which is in good agreement with the experimental results (Table 2, entry 1). Moreover, the effective blockage of the (1Si,3Re) prochiral face by the catalytic system is compatible with the energetic difference of 1.8 kcal/mol between TS1 and TS2. This difference in favor of TS1 is related to the lower energy required to deform the geometry of the complex formed by the chiral ligand 18 and the N-metalated azomethine ylide. This initial geometry is modified to that of the TS. In addition, this geometry change
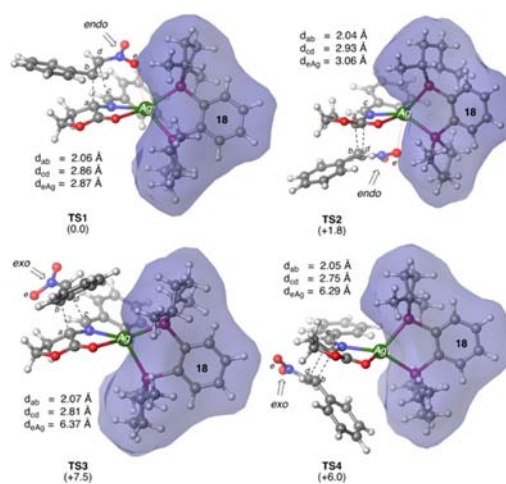
Figure 2. Main geometric features and relative energies (kcal/mol) of the computed transition structures associated with the first step of the reaction between 8 and azomethine ylide (R,R)-MeDuPhos-Ag·7a computed at M06(PCM)/6-31G*&LanL2DZ//B3LYP(PCM)/6-31G*&LanL2DZ. Bond lengths are given in Å. Blue surfaces represent the solvent-accessible surface with a probe radius of 1.9 Å.

minimizes the TS steric repulsion between the incoming nitroalkene and the catalytic system. This computed energetic difference is associated with a theoretical er of 96:4, also in perfect agreement with the experimental evidence.

The complete reaction mechanism that yields the cycloadduct 9aa was further analyzed. The main geometrical features of the second transition structure TS5 and the energetic profile are depicted in Figure 3. The computed Gibbs activation barrier
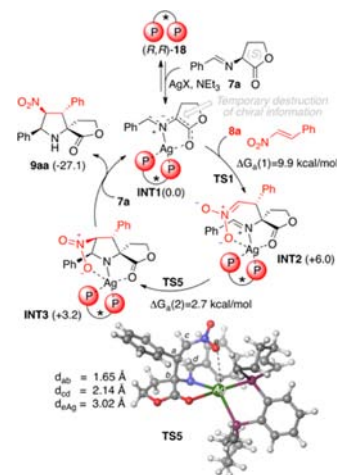
Figure 3. Main geometric features of the second transition structure and relative energies (in kcal/mol) of the profile associated with the reaction between 8 and azomethine ylide INT1 to yield 9aa computed at the M06(PCM)/6-31G*&LanL2DZ//B3LYP(PCM)/6-31G*&LanL2DZ level of theory. Bond lengths are given in Å.

associated with the second step was ca. 7 kcal/mol lower than that associated with the first step. However, formation of the mayor cycloadduct is slightly endergonic. Therefore, the final equilibrium is the driving force of the reaction because it ensures the release of 9aa and the recovery of the reactive ylide complex.

The relative configuration of major stereoisomers endo-9, deduced by NOE experiments and correlation with the chemical shifts and coupling constants previously reported for the racemic

products,[14] was in agreement with the absolute configuration revealed by both the most favored computed structure and X-ray diffraction analysis of *endo*-**9ga**.[27]

In conclusion, an efficient method for the synthesis of spiranic cycloadducts *endo*-**9** from α-imino γ-lactones has been achieved. (*R,R*)-MeDuPhos **18**·AgF was the most efficient in acting as a bifunctional catalyst because the fluoride behaves as base. The *endo*-diastereoisomers were obtained in both high enantio- and diastereomeric ratios.[28] DFT calculations were found to be a crucial tool to clarify the absolute configuration of these cycloadducts, which was confirmed later by X-ray diffraction analysis.

■ ASSOCIATED CONTENT

Ⓢ Supporting Information

The Supporting Information is available free of charge on the ACS Publications website at DOI: 10.1021/acs.orglett.6b01273.

> Experimental details, characterization data, and NMR spectra for new compounds (PDF)
> Computational data and X-RD analysis (CIF)

■ AUTHOR INFORMATION

Corresponding Authors

*E-mail: jmsansano@ua.es.
*E-mail: fp.cossio@ehu.es.

Notes

The authors declare no competing financial interest.

■ ACKNOWLEDGMENTS

■ REFERENCES

(1) Nájera, C.; Sansano, J. M. *Curr. Top. Med. Chem.* **2014**, *14*, 1271.

(2) San Sebastián, E.; Zimmerman, T.; Zubia, A.; Vara, Y.; Martin, E.; Sirockin, F.; Dejaegere, A.; Stote, R. H.; López, X.; Pantoja-Uceda, D.; Valcárcel, M.; Mendoza, L.; Vidal-Vanaclocha, F.; Cossío, F. P.; Blanco, F. J. *J. Med. Chem.* **2013**, *56*, 735.

(3) Zubia, A.; Mendoza, L.; Vivanco, S.; Aldaba, E.; Carrascal, T.; Lecea, B.; Arrieta, A.; Zimmerman, T.; Vidal-Vanaclocha, F.; Cossío, F. P. *Angew. Chem., Int. Ed.* **2005**, *44*, 2903.

(4) Narayan, R.; Bauer, J. O.; Strohmann, C.; Antonchick, A. P.; Waldmann, H. *Angew. Chem., Int. Ed.* **2013**, *52*, 12892.

(5) Puerto-Galvis, C. E.; Kouznetsov, V. V. *Org. Biomol. Chem.* **2013**, *11*, 7372.

(6) Tripathi, R. P.; Bisht, S. S.; Pandey, V. P.; Pandey, S. K.; Singh, S.; Sinha, S. K.; Chaturvedi, V. *Med. Chem. Res.* **2011**, *20*, 1515.

(7) Conde, E.; Bello, D.; de Cózar, A.; Sánchez, M.; Vázquez, M. A.; Cossío, F. P. *Chem. Sci.* **2012**, *3*, 1486.

(8) Ruíz-Olalla, A.; Retamosa, M. d. G.; Cossío, F. P. *J. Org. Chem.* **2015**, *80*, 5588.

(9) Cossío, F. P.; Retamosa, M. d. G.; Larumbe, A.; Zubia, A.; Bello, T.; Vara, Y. I.; Masdeu, C.; Aldaba, E. Patent WO2015/124663, 2015.

(10) (a) Han, M.-Y.; Jia, J.-Y.; Wang, W. *Tetrahedron Lett.* **2014**, *55*, 784. (b) Suga, H.; Itoh, K. In *Methods and Applications of Cycloaddition Reactions in Organic Syntheses*; Nishiwaki, N., Ed.; Wiley: Weinheim, 2014; pp 175−204 and references cited therein.

(11) Conde, E.; Rivilla, I.; Larumbe, A.; Cossío, F. P. *J. Org. Chem.* **2015**, *80*, 11755.

(12) For recent and representative examples of sterically congested systems generated by 1,3-DC, see: (a) Yang, W.-L.; Liu, Y.-Z.; Luo, S.; Yu, X.; Fossey, J. S.; Deng, W.-P. *Chem. Commun.* **2015**, *51*, 9212. (b) Bharitkar, Y. P.; Das, M.; Kumari, N.; Kumari, M. P.; Hazra, A.; Bhayye; Sagar, S.; Natarajan, R.; Shah, S.; Chatterjee, S.; Mondal, N. B. *Org. Lett.* **2015**, *17*, 4440.

(13) For representative references involving homoserine derived imino esters, see: (a) Teng, H.-L.; Huang, H.; Wang, R. *Chem. - Eur. J.* **2012**, *18*, 12614. (b) Liu, T.; He, Z.; Tao, H.; Wang, C.-J. *Chem. - Eur. J.* **2012**, *18*, 8042. (c) Liu, T.-L.; Wei, L.; Zhou, X.; Tao, H.-Y.; Wang, C.-J. *Org. Lett.* **2013**, *15*, 2250. (d) Wang, L.; Shi, X.-M.; Dong, W.-P.; Zhu, L.-P.; Wang, C.-J. *Chem. Commun.* **2013**, *49*, 3458.

(14) Grigg, R.; Kilner, C.; Sarker, M. A. B.; Orgaz de la Cierva, C.; Dondas, A. H. *Tetrahedron* **2008**, *64*, 8974.

(15) Fang, X.; Dong, X.-Q.; Wang, C. J. *Tetrahedron Lett.* **2014**, *55*, 5660.

(16) See, for instance: (a) Bucio-Cano, A.; Reyes-Arellano, A.; Correa-Basurto, J.; Bello, M.; Torres-Jaramillo, J.; Salgado-Zamora, H.; Curiel-Quesada, E.; Peralta-Cruz, J.; Ávila-Sorrosa, A. *Bioorg. Med. Chem.* **2015**, *23*, 7565. (b) Brameyer, S.; Bode, H. B.; Heermann, R. *Trends Microbiol.* **2015**, *23*, 521.

(17) For recent reviews of asymmetric 1,3-DC, see: (a) Adrio, J.; Carretero, J. C. *Chem. Commun.* **2011**, *47*, 6784. (b) Adrio, J.; Carretero, J. C. *Chem. Commun.* **2014**, *50*, 12434. (c) Nájera, C.; Sansano, J. M. *J. Organomet. Chem.* **2014**, *771*, 78. (d) Hashimoto, T.; Maruoka, K. *Chem. Rev.* **2015**, *115*, 5366.

(18) Nájera, C.; Sansano, J. M. *Chem. Rec.* **2016**, DOI: 10.1002/tcr.201500283.

(19) For very recent enantioselective 1,3-DC between imino esters and nitroalkenes see: (a) Kimura, M.; Matsuda, Y.; Koizumi, A.; Tokumitsu, C.; Tokoro, Y.; Fukuzawa, S.-i. *Tetrahedron* **2016**, *72*, 2666−2670. (b) Sun, Q.; Li, X.-Y.; Su, J.; Zhao, L.; Ma, M.; Zhu, Y.; Zhao, Y.; Zhu, R.; Yan, W.; Wang, K.; Wang, R. *Adv. Synth. Catal.* **2015**, *357*, 3187−3196. (c) Pascual-Escudero, A.; González-Esguevillas, M.; Padilla, S.; Adrio, J.; Carretero, J. C. *Org. Lett.* **2014**, *16*, 2228−2231.

(20) Castelló, L. M.; Nájera, C.; Sansano, J. M.; Larrañaga, O.; de Cózar, A.; Cossío, F. P. *Synthesis* **2015**, *47*, 934.

(21) Mancebo-Aracil, J.; Nájera, C.; Sansano, J. M. *Tetrahedron: Asymmetry* **2015**, *26*, 674; *Synfacts* **2015**, *11*, 1065.

(22) The monomeric species (*R,R*)-Me-DuPhos **18**·AgF can be assumed as the catalyst because any NLE was detected.

(23) (a) Parr, R. G.; Yang, W. *Density-Functional Theory of Atoms and Molecules*; Oxford University Press: Oxford, New York, 1989. (b) Lee, C.; Yang, W.; Parr, R. G. *Phys. Rev. B: Condens. Matter Mater. Phys.* **1988**, *37*, 785. (c) Becke, A. D. *J. Chem. Phys.* **1993**, *98*, 1372. (d) Becke, A. D. *J. Chem. Phys.* **1993**, *98*, 5648. (e) Hay, P. J.; Wadt, W. R. *J. Chem. Phys.* **1985**, *82*, 299. (f) *Gaussian 09*, revision B.01; Gaussian, Inc.: Wallingford, CT, 2009.

(24) Nájera, C.; Retamosa, M. G.; Sansano, J. M.; de Cózar, A.; Cossío, F. P. *Eur. J. Org. Chem.* **2007**, *2007*, 5038.

(25) De Cózar, A.; Cossío, F. P. *Phys. Chem. Chem. Phys.* **2011**, *13*, 10858.

(26) (a) Vivanco, S.; Lecea, B.; Arrieta, A.; Prieto, P.; Morao, I.; Linden, A.; Cossío, F. P. *J. Am. Chem. Soc.* **2000**, *122*, 6078. (b) Ayerbe, M.; Arrieta, A.; Cossío, F. P.; Linden, A. *J. Org. Chem.* **1998**, *63*, 1795.

(27) Crystal structure was deposited at the Cambridge Crystallographic Data Centre: CCDC 1477484.

(28) In general *exo*-adducts are obtained in the reactions involving nitroalkenes and metallo-azomethine ylides.